STABLE-SPAM: HOW TO STABLY TRAIN LARGE LANGUAGE MODELS IN 4-BIT

Anonymous authorsPaper under double-blind review

000

001

002003004

010 011

012

013

014

015

016

017

018

019

021

023

025

026

027

028

029

031

032

034

035

037

040

041

042

043

044

046

047

051 052

ABSTRACT

This paper comprehensively evaluates several recently proposed optimizers for 4-bit training, revealing that low-bit precision amplifies sensitivity to learning rates and often causes unstable gradient norms, leading to divergence at higher learning rates. Among these, SPAM, a recent optimizer featuring momentum reset and spike-aware gradient clipping, achieves the best performance across various bit levels, but struggles to stabilize gradient norms, requiring careful learning rate tuning. To address these limitations, we propose Stable-SPAM, which incorporates enhanced gradient normalization and clipping techniques. In particular, Stable-SPAM (1) adaptively updates the clipping threshold for spiked gradients by tracking their historical maxima; (2) normalizes the entire gradient matrix based on its historical l_2 -norm statistics; and (3) inherits momentum reset from SPAM to periodically reset the first and second moments of Adam, mitigating the accumulation of spiked gradients. Extensive experiments show that Stable-SPAM effectively stabilizes gradient norms in 4-bit LLM training, consistently delivering superior performance compared to Adam and SPAM across model sizes from LLaMA-130M to LLaMA-7B. Notably, our 4-bit LLaMA-1B model trained with Stable-SPAM outperforms Adam by up to 3.1 perplexity. Furthermore, when both models are trained in 4-bit, Stable-SPAM achieves the same loss as Adam while requiring only about half the training steps. Code is submitted.

1 Introduction

Recently, several advanced optimizers have been proposed, claiming to either outperform the widely used Adam optimizer or achieve comparable performance at reduced costs in the context of Large Language Models (LLMs). Given the massive size of LLMs, reducing the memory footprint of Adam has become a key objective in this line of research (Shazeer & Stern, 2018; Chen et al., 2024; Zhang et al., 2024a; Zhao et al., 2024a; Zhang et al., 2024b; Ma et al., 2024). Another area of focus is addressing the challenges of instability in LLM training. For instance, Huang et al. (2025) proposed SPAM which incorporates momentum reset and spike-aware gradient clip (SpikeClip) to mitigate the adverse effects of loss spikes. Zhao et al. (2024b) studied the stability of various optimizers to hyperparameters with BF16. These optimizers are predominantly evaluated using the standard BF16 precision, which is a practical option for real-world LLM training (Touvron et al., 2023; Li et al., 2023). With the growing shift toward low-bit precisions such as FP8 and FP4 in LLMs due to their significant cost-saving potential (Liu et al., 2024; Lee et al., 2024; Peng et al., 2023; Xi et al., 2023), it is crucial to investigate whether their effectiveness persists under lower-bit precisions. For the newly proposed optimizers to be economical, their training with low-bit precisions should be similarly robust to hyperparameter choice as trained using higher precision.

This paper provides a comprehensive evaluation of the effectiveness and robustness of learning rate choices across various recent optimizers, including Adam (Kingma, 2014), Adafactor (Shazeer & Stern, 2018), Adam-mini (Zhang et al., 2024a), and SPAM (Huang et al., 2025), when training with 4-bit weights and activations. Our study reveals several key observations:

* All evaluated optimizers exhibit increased sensitivity to learning rate choices during 4-bit training, often diverging quickly when larger learning rates are used as shown in Figure 2.

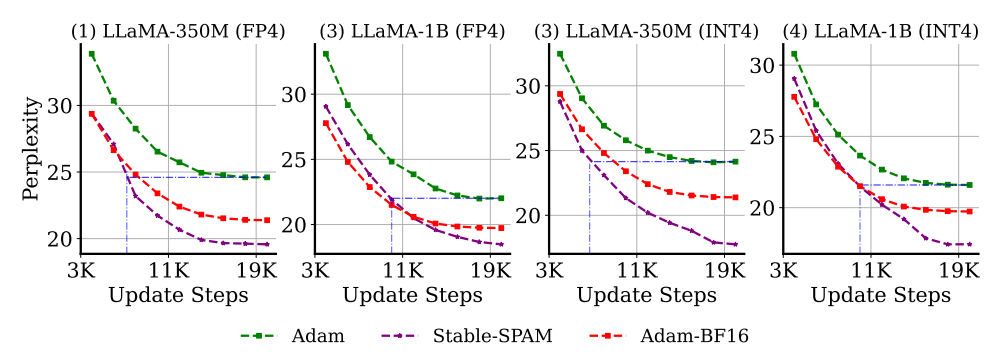


Figure 1: **Effectiveness of Stable-SPAM in 4-bit LLM training.** Experiments are conducted with LLaMA-130M/350M/1B models on C4 Dataset. **Adam-BF16** denotes that the model is trained with BF16 by Adam. Perplexity on validation set is reported.

- * SPAM (Huang et al., 2025) consistently achieves the lowest evaluation loss across various bit levels but requires careful learning rate tuning. Adafactor is surprisingly robust to learning rate choices, even outperforming Adam in this regard.
- * Our analysis of the training dynamics in Figure 4 reveals that 4-bit training often exhibits extremely unstable gradient norms, often accompanied by spikes, compared to BF16. This behavior can result in loss spikes and, in some cases, even training divergence with relatively larger learning rates.
- * While SpikeClip introduced in SPAM mitigates the unstable gradient norms caused by 4-bit training to a certain extent, it falls short of fully preventing training divergence, as shown in Figure 3.

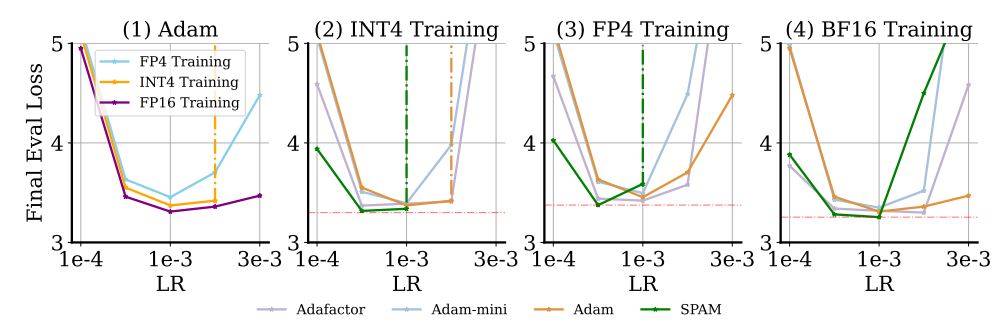


Figure 2: Learning instability of existing optimizers during 4-bit training. Final validation loss is reported. The vertical dotted line indicates that the model cannot be trained further as increasing the learning rate, i.e. Training loss becomes NaN. Red dashed horizontal lines indicate the best performance achieved.

Despite its sensitivity to learning rate selection, SPAM (Huang et al., 2025) consistently achieves the lowest evaluation loss across various bit levels, making it an ideal foundation for improvement. Building on this, we introduce Stable-SPAM to address the instability challenges associated with low-precision training of LLMs. Stable-SPAM retains the superior performance of SPAM¹ while improving stability, offering a significant advancement in low-precision optimization.

Specifically, beyond the original momentum reset operation in SPAM, Stable-SPAM introduces two key techniques: Adaptive Spike-Aware Clipping (AdaClip), which enables adaptive clipping of spiked gradients, followed by Adaptive Gradient Norm (AdaGN), which normalizes the entire gradient matrix based on its historical l_2 norm statistics. Our analysis demonstrates that these enhancements effectively stabilize the gradient norm of 4-bit training, achieving better performance than Adam and SPAM. Furthermore, when both models are trained in 4-bit, Stable-SPAM achieves the same loss as Adam while requiring only about half the training steps.

¹Nevertheless, results in Table 3 show that our proposed techniques also improve the performance of other optimizers.

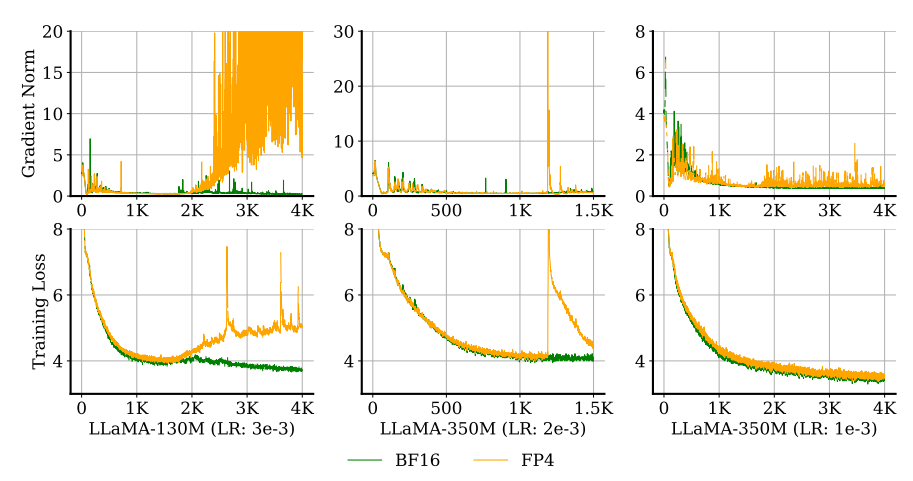


Figure 4: **Training loss and gradient norm spikes under 4-bit Training.** Experiments are conducted under the same training configuration with LLaMA-130M/350M.

2 4-BIT TRAINING STABILITY INVESTIGATION

Recent studies (Zhao et al., 2024b; Wortsman et al., 2023b; Huang et al., 2025; Takase et al., 2023; Wortsman et al., 2023b) have investigated stability challenges in large language model (LLM) training, including issues such as learning rate instability, gradient spikes, and loss spikes. In this section, we extend the evaluation by analyzing the stability of various optimization algorithms under a 4-bit LLM training setting. Following the experimental setup outlined in Wortsman et al. (2023b); Zhao et al. (2024b), we evaluate the final performance using a range of learning rates from 1e-4 to 3e-3. This evaluation includes two widely used optimizers, Adam (Kingma, 2014) and Adafactor (Shazeer & Stern, 2018), as well as two recently proposed methods, Adammini (Zhang et al., 2024a) and SPAM (Huang et al., 2025). Additionally, we monitor both the

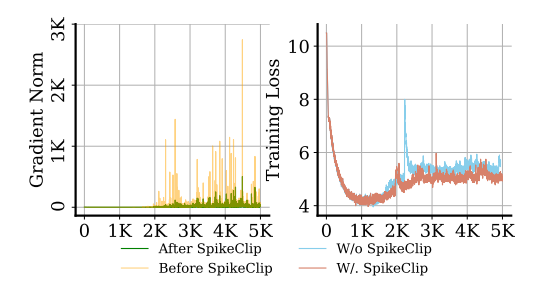


Figure 3: Ineffectiveness of SpikeClip (Huang et al., 2025) in preventing training divergence. Left: gradient norms before and after performing gradient spike clip. Right: training loss with and without applying gradient spike clip. Models are trained by Adam based on LLaMA-130M.

global gradient norm and training loss throughout the 4-bit LLM training process. The global gradient norm is defined as follows: $\sqrt{\sum_{i=0}^{N}\|g_i\|_2^2}$ where N is the number of layers in model and g_i denotes the gradient of i-th layer. The experiments are conducted on the LLaMA-130M/350M models using the C4 dataset and showed in Figure 2 and Figure 4. We observe:

- **1.1 Lower-bit training exhibits reduced learning rate stability.** As illustrated in Figure 2, the final evaluation loss for 4-bit training increases significantly with larger learning rates, whereas BF16 training exhibits a more stable performance across different learning rates. This indicates that 4-bit training is more sensitive and less stable in terms of learning rate.
- **Q** Lower-bit training suffers more loss spikes and gradient norm spikes. Figure 4 illustrates this phenomenon by comparing the training loss and gradient norm curves of LLaMA-130M and LLaMA-350M trained under BF16 and FP4 (E1M2) precision, using various learning rates. We observe that BF16 training remains stable, but FP4 training exhibits significant loss spikes, which occur on both model sizes. Furthermore, these loss spikes are consistently accompanied by gradient norm explosions.
- SPAM performs the best in 4-bit training but needs careful learning rate tuning. As shown in Figure 2, SPAM achieves the lowest eval loss among various optimizers in INT4 or FP4 with the

optimal learning rate. However, its validation loss either diverges to NaN or sharply increases as the learning rate rises.

Although SPAM can partially mitigate gradient spikes, it fails to prevent training divergence entirely. We monitor the training loss and gradient norm after applying the spike clipping technique (SpikeClip) proposed in SPAM. SpikeClip detects and mitigates gradient outliers by leveraging the second moment of gradients. Specifically, it follows the expression: $g_i = \text{sign}(g_i) \cdot \sqrt{\theta V_i}$ under the condition $\frac{g_i^2}{V_i} > \theta$ where g_i, V_i, θ are the gradient, second moment and pre-defined threshold (5000 used by default in their paper) respectively. We observe that although SpikeClip can partially mitigate loss spikes, it fails to prevent training divergence entirely. A plausible explanation is that SpikeClip performs element-wise clipping using a fixed threshold, which may be insufficient when all gradient components increase simultaneously. In such cases, the overall gradient norm can remain large despite the absence of extreme outliers, since SpikeClip only targets individual large values rather than accounting for the collective magnitude. This limitation is evident in Figure 3, where the gradient norm explosions remain elevated even after applying SpikeClip.

STABLE-SPAM

162

163

164

166

167

168

169

170

171

172

173

174

175

176 177

178 179

181

182

183

185

186

187

188

189

190

191 192 193

194

196 197

199

200

201

202

203

204

205

206

207

208

209

210

211 212

213

214

215

To address the training instability in 4-bit training, we propose Stable-SPAM, a stabilized spike-aware Adam optimizer. Apart from the momentum reset inherited from the original SPAM, Stable-SPAM introduces two techniques: Adaptive Gradient Norm (AdaGN) and Adaptive Spike-Aware Clipping (AdaClip), which we will explain in detail. The pseudocode is provided in Appendix I.

Adaptive Gradient Norm (AdaGN). As we can observe in Figures 4 and 3, spikes in training loss and instances of training divergence usually align with abrupt surges in the gradient norm, consistent with findings in Takase et al. (2023); Huang et al. (2025). To address these training instabilities, we propose AdaGN, a method that stabilizes gradients by adaptively scaling them based on their historical l_2 norm statistics. To better track the dynamics of the gradient norm during training, we leverage the idea of Adam by maintaining moving averages of both the first and second moments of the gradient norm. Concretely, we compute and update the moving averages of the gradient norm (m_{norm}, v_{norm}) , then use them to derive a normalized gradient:

$$g_{\text{norm}} = ||g_t||_2, \quad m_{\text{norm}} = \gamma_1 m_{\text{norm}} + (1 - \gamma_1) g_{\text{norm}},$$
 (1)

$$g_{\text{norm}} = ||g_t||_2, \quad m_{\text{norm}} = \gamma_1 m_{\text{norm}} + (1 - \gamma_1) g_{\text{norm}},$$

$$v_{\text{norm}} = \gamma_2 v_{\text{norm}} + (1 - \gamma_2) g_{\text{norm}}^2, \quad \hat{g}_t = \frac{g_t}{g_{\text{norm}}} \cdot \frac{m_{\text{norm}}}{\sqrt{v_{\text{norm}}} + \epsilon}.$$
(2)

where \hat{g}_t is the normalized gradient, γ_1 and γ_2 are momentum coefficients and ϵ is small constant for numerical stability. By rescaling g_t with a ratio of its historical mean norm m_{norm} to the square root of its historical second moment $\sqrt{v_{norm}}$, AdaGN mitigates abrupt gradient norm spikes. Note that as the gradient norm g_{norm} is essentially a scalar for an entire layer, the additional parameter overhead introduced by AdaGN is negligible, i.e., two extra parameters per layer.

Adaptive Spike-Aware Clipping. (AdaClip) Different from the spike gradient clipping technique in Huang et al. (2025), which sets a fixed clipping threshold, we propose an adaptive clipping approach, i.e., AdaClip. The core idea is to dynamically adjust the clipping threshold by tracking the maximum gradient magnitude observed over time, rather than relying on a pre-defined fixed value. Concretely, let g_t be the gradient at time step t. We first compute g_{max} , the maximum absolute gradient value across all parameters. Then, we update the threshold $T_{threshold}$ with an exponential moving average that incorporates g_{max} . Finally, any entries of g_t that exceed $T_{\text{threshold}}$ are rescaled to maintain stability. The procedure is formally expressed as follows:

$$g_{\text{max}} = \max_{i} (|g_t[i]|), \quad T_{\text{threshold}} = \gamma_3 \cdot T_{\text{threshold}} + (1 - \gamma_3) \cdot g_{\text{max}},$$
 (3)

$$Mask_{spikes} = (g_t > T_{threshold}), \quad g_t[Mask_{spikes}] = \frac{g_t[Mask_{spikes}]}{g_{max}} \times T_{threshold}, \tag{4}$$

where $\gamma_3 \in [0,1]$ controls the weight of the moving average. When γ_3 is large, $T_{\text{threshold}}$ responds more slowly to new gradient maxima, leading to more stable updates. When γ_3 is small, it adapts more quickly to sharp changes in gradient magnitude.

Table 1: Performance of INT4/FP4 pre-training with LLaMA (C4). All optimizers are trained with weight decay=0 except for AdamW which used its default value: 0.01.

Perplexity	INT4 Training			FP4 Training		
Гегріскі	130M	350M	1B	130M	350M	1B
AdamW(WD=0.01)	25.73	18.64	18.01	28.12	20.10	18.76
Adam	26.40	19.21	18.39	28.9	20.64	19.11
Adam+GradClip	26.30	18.47	17.82	28.27	20.08	18.64
Adafactor	25.11	18.35	17.64	26.89	19.67	18.33
SPAM	25.03	18.39	17.38	26.78	19.56	18.02
Stable-SPAM	24.33	17.20	16.27	26.31	18.08	15.92
Training Tokens	2.2B	6.6B	7.7B	2.2B	6.6B	7.7B

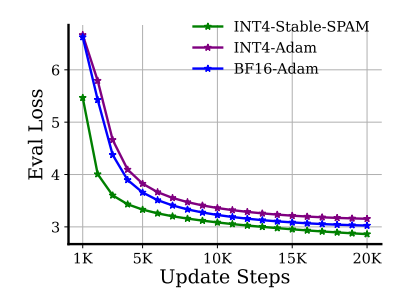


Figure 5: Training curves of LLaMA-7B trained with 4 bit.

Momentum Reset (MoRet). Following Huang et al. (2025), we adopt momentum reset (MoRet) to periodically reset the accumulated first and second moments in Adam. The effectiveness of MoRet lies in addressing the negative effects of gradient spikes, which can inflate the first and second moments of Adam. Since Adam uses exponential moving averages to track their historical information, these inflated values caused by spiked gradients can have prolonged detrimental effects (Huang et al., 2025) on moments. By resetting the momentum terms at fixed intervals (ΔT), MoRet mitigates the lasting influence of unusually large gradients, enabling more stable optimization.

4 EXPERIMENTS

To demonstrate the efficacy of the proposed Stable-SPAM, we conduct extensive experiments with various sizes of the LLaMA model on the C4 dataset.

Baselines. We adopt five popular optimizers as our baselines including Adam (Kingma, 2014), AdamW (Loshchilov & Hutter, 2017), Adafactor (Shazeer & Stern, 2018), Lion (Chen et al., 2024), Adam-mini (Zhang et al., 2024a) and SPAM (Huang et al., 2025). Among these, Adam and Adafactor are well-established and widely used, while Adam-mini and SPAM have been introduced more recently. Besides, we also include gradient clipping (Goodfellow, 2016) (GradClip) in conjunction with Adam as an additional baseline. All optimizers are applied without using weight decay, except for AdamW, which employs its default setting of 0.01.

Experimental Setup. Following Lialin et al. (2023); Zhao et al. (2024a), we train LLaMA-based architectures ranging from 60M to 1B parameters. Each architecture is configured with RMSNorm Shazeer (2020) and SwiGLU activations Zhang & Sennrich (2019). For every model size, we keep the same set of hyperparameters across methods and vary only the learning rate. We sweep over learning rates from 1×10^{-4} to 1×10^{-3} , incrementing by 2×10^{-4} for each optimizer. Following the settings in Takase et al. (2023); Huang et al. (2025), we set the threshold to 1 for the GradClip baseline. For Adafactor, we adopt the hyperparameters from the original paper Shazeer & Stern (2018), where $\epsilon_1=10^{-30}$, $\epsilon_2=10^{-3}$, and d=1.0. The hyperparameters for SPAM are configured based on the settings in Huang et al. (2025), with reset intervals set to 500, learning rate warmup steps to 150, and the GSS threshold to 5000. For Stable-SPAM, we set $\gamma_1=0.7$, $\gamma_2=0.9$ and $\theta=0.999$ for 4-bit LLM training and $\gamma_1=0.85$, $\gamma_2=0.9999$ and $\gamma_3=0.999$ for BF16 training. Detailed descriptions of our task setups and hyperparameters are provided in the Appendix B.

4.1 Performance of 4-bit LLM Training

To evaluate the performance of Stable-SPAM in 4-bit LLM training, we conduct experiments using both FP4 (E1M2: 1-bit exponent, 2-bit mantissa)² and INT4 (4-bit integer) quantization-aware training strategies. The training curves of various LLaMA models on the C4 dataset are presented in Figure 1, and the final perplexity results are summarized in Table 1.

 $^{^2}$ The FP4 quantization and dequantization procedures follow the implementation described in https://arxiv.org/pdf/2310.16836.

We observe that 4-bit training leads to a significant performance drop compared to BF16 training. As shown in Table 1, the perplexity gap between BF16 (Adam) and INT4/FP4 (Adam) exceeds 1.5 across all model sizes, highlighting the challenges of reduced precision. Figure 1 shows that Stable-SPAM consistently outper-forms Adam by a significant margin in 4-bit scenarios. Table 1 further demonstrates that Stable-SPAM outperforms other ad-vanced optimizers, such as Adafactor and

Table 2: Comparison among various optimizers on BF16 training. Perplexity is reported. All optimizers are trained with weight decay=0 except for AdamW which used its default value: 0.01.

Optimizer	60M	130M	350M	1B
Adam-mini	34.10	24.85	19.05	16.07
AdamW (WD=0.01)	33.23	24.27	18.39	15.318
Adam	34.09	24.91	18.77	16.13
Adam + GradClip	33.33	24.88	18.51	15.22
Adafactor	32.57	23.98	17.74	15.19
SPAM	30.46	23.36	17.42	14.66
Stable-SPAM	28.84	22.21	16.85	13.90
Training Tokens	1.1B	2.2B	6.6B	11.6B

SPAM. Among the baselines, incorporating

GradClip reduces perplexity, while Adafactor and SPAM both outperform the simple application of GradClip. Stable-SPAM is able to match Adam's performance with half the tokens in 4-bit training. As illustrated in Figure 1, Stable-SPAM achieves the same perplexity as Adam in approximately half the training steps. Notably, Stable-SPAM performs particularly well with larger models, such as LLaMA-350M and LLaMA-1B, showcasing its strong potential for large-scale training. This is likely because large-scale, low-precision training is more susceptible to instability issues (Fishman et al., 2024), making stabilized training approaches like Stable-SPAM especially beneficial.

4.2 Scale up to 7B Model

We further validate Stable-SPAM on a larger model with 7B parameters. Specifically, we compare Stable-SPAM and Adam under INT4 training and present the training curves over 20K update steps. As shown in Figure 5, Stable-SPAM consistently outperforms Adam on this large-scale training scenario.

4.3 Performance of Extremely Low-Precision Training

To evaluate the performance of Stable-SPAM under extremely low-precision training, we conducted experiments on LLaMA-350M using A2W2 (INT2), A3W3 (INT3), and A4W4 (INT4) configurations. The final validation loss is presented in Figure 4. The results indicate that Stable-SPAM consistently outperforms Adam across all low-precision settings.

4.4 Performance of BF16 LLM Training

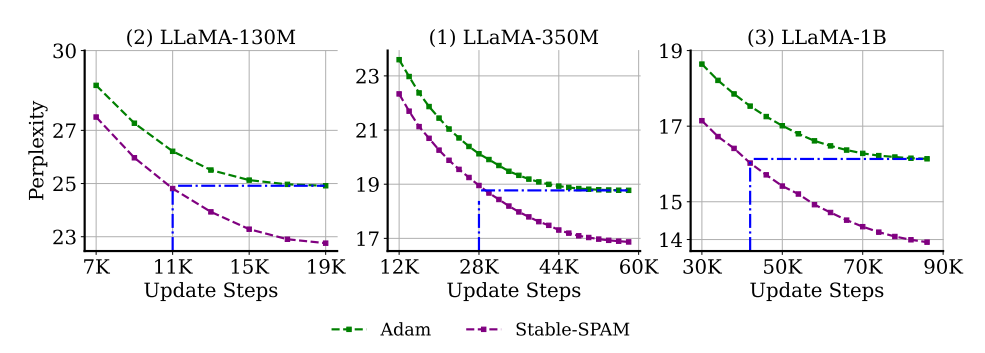


Figure 6: **Performance of BF16 training with various model sizes.** Experiments are based on LLaMA models trained on C4 Dataset.

To further evaluate the efficacy of Stable-SPAM, we conducted experiments on various LLaMA model sizes following the standard BF16 training in Zhao et al. (2024a). The experiments are based on C4 dataset. The training curves and final perplexity values are presented in Figure 6 and Table 2, respectively. Table 2 highlights that Stable-SPAM consistently delivers superior performance across different model sizes, surpassing the second-best optimizer with significant improvements. Furthermore, Figure 6 illustrates that Stable-SPAM achieves the same performance as Adam in only half the training steps or even fewer for LLaMA-350M and LLaMA-1B, validating its ability to

match Adam's performance while requiring significantly fewer tokens under BF16 LLM training. The above results demonstrate that the promise of Stable-SPAM not only holds for low-precision LLM training but also holds for the standard BF16 training.

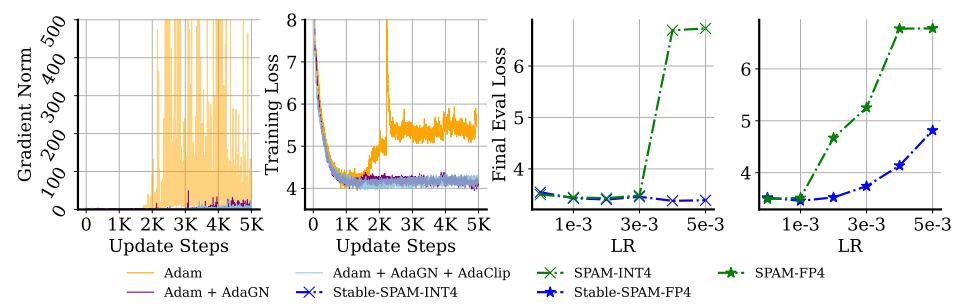


Figure 7: **Effectivess of AdaGN and AdaClip on stabilizing FP4 LLM training.** The left two figures use LLaMA-130M (LR = 3e-3), and the right two figures use LLaMA-60M.

4.5 Integration with Other Optimizers

Table 3: Improvements from AdaGN and AdaClip on Lion and Adam-mini optimizers. Experiments are based on LLaMA-60M/130M with 4-Bit training.

Optimizers	INT4	Training	FP4 Training	
Optimizers	60M	130M	60M	130M
Lion	39.36	35.28	39.89	34.20
Lion+AdaGN+AdaClip	38.49	29.40	36.75	31.63
Adam-mini	34.84	29.79	36.37	32.95
Adam-mini+AdaGN+AdaClip	34.61	29.65	34.65	32.39
Training Tokens		1.1	В	



Table 4: **StableSPAM under Extremely Low-Precision Training.** Experiments are conducted with 350M models on C4 Dataset.

Although AdaGN and AdaClip are proposed specifically for Stable-SPAM, one may wonder, "Can AdaGN and AdaClip also be compatible with other optimizers?" To answer this question, we applied AdaGN and AdaClip to two recently published optimizers: Lion (Chen et al., 2024) and Adam-mini (Zhang et al., 2024a). We conducted comparative experiments using Lion and Adam-mini alone, as well as in combination with AdaGN and AdaClip, under a 4-bit training setting. These experiments were performed on LLaMA-60M/130M models with the C4 dataset.

The results in Table 3 show that AdaGN and AdaClip consistently enhance the performance of both Lion and Adam-mini under FP4 and INT4 training settings, across LLaMA-60M and LLaMA-130M model sizes. Notably, on LLaMA-130M with INT4 training, Lion achieves a perplexity improvement of up to 5.88, and Adam-mini on LLaMA-60M under FP4 training sees an improvement of 1.72. These improvements underscore the broad applicability and effectiveness of the proposed AdaGN and AdaClip methods.

4.6 EFFECT ON STABILIZING TRAINING

To validate the effectiveness of our proposed AdaGN and AdaClip techniques in stabilizing the LLM training process, Firstly, we compared the training loss and gradient norm curves across three settings: using Adam alone, using Adam with AdaGN, and using Adam with both AdaGN and AdaClip. Our experiments employed LLaMA-130M with a learning rate of 3e-3 under an FP4 training setting. As shown in Figure 7, training solely with Adam leads to divergence in the training loss and frequent spikes in the gradient norm. However, once AdaGN is introduced, the training loss converges, and the gradient norm is noticeably reduced. Adding AdaClip on top of AdaGN further decreases the gradient norm and yields a smoother training loss curve. Secondly, we present the final performance across a range of learning rates, from 5×10^{-4} to 5×10^{-3} , evaluated on LLaMA-60M under both FP4 and INT4 training settings. The results in Figure 7 show that Stable-SPAM produces a significantly flatter curve, highlighting its stability across varying learning rates. These

results demonstrate the effectiveness of the proposed AdaGN and AdaClip techniques in achieving a more stable and consistent training process.

4.7 ABLATION STUDY

To validate the effectiveness of the three components, MoRet, AdaGN, and AdaClip, in Stable-SPAM, we conduct a comprehensive ablation study. Specifically, we take two approaches: (1) We iteratively incorporate MoRet, AdaGN, and AdaClip into the Adam optimizer to measure their individual and combined improvements under both FP4 and BF16 training settings. (2) We replace AdaClip with SpikeClip Huang et al. (2025) and AdaGN with Grad-

Table 5: **Ablations on Stable-SPAM.** Experiments are based on LLaMA-60M and C4.

Optimizer	FP4	BF16
Adam	35.47	34.09
Adam + MoRet	32.4	31.47
Adam + MoRet + AdaClip	31.97	30.29
Adam + MoRet + AdaGN	32.26	28.96
Adam + MoRet + AdaGN + AdaClip (Stable-SPAM)	31.40	28.84
Adam + MoRet + AdaGN + SpikeClip Huang et al. (2025)	32.01	28.90
Adam + MoRet + GradClip Goodfellow (2016)+AdaClip	31.95	29.87
Adam + MoRet+AdaGN+AdaClip (Stable-SPAM)	31.40	28.84
Training Tokens	1.	1B

Clip Goodfellow (2016) to further assess the unique contributions of our proposed components. The results, summarized in Table 5, reveal the following observations: MoRet consistently improves performance across both FP4 and BF16 settings. Under both FP4 training, AdaGN alone shows limited improvement. However, when combined with AdaClip, it substantially reduces final perplexity. Conversely, in the BF16 setting, AdaGN alone yields considerable performance gains, but adding AdaClip offers limited improvement. This discrepancy may stem from the higher frequency of extreme element-wise gradient spikes in this FP4 training experiments, which necessitates AdaClip to correct biased update directions effectively. Finally, replacing AdaClip with SpikeClip Huang et al. (2025) and AdaGN with GradClip Goodfellow (2016) results in increased perplexity, further validating the efficacy of our proposed AdaGN and AdaClip.

4.8 Hyper-Parameter Analysis

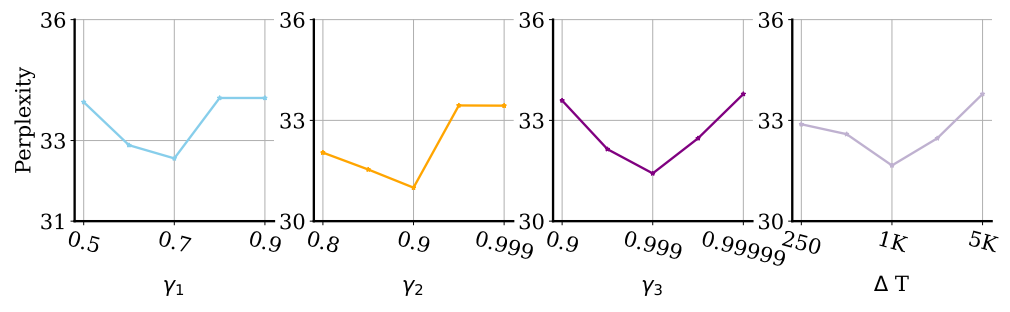


Figure 8: **Hyper-parameter Analysis.** Experiments are conducted with FP4 training on LLaMA-60M and C4 with 1.1B tokens.

Stable-SPAM introduces four hyperparameters: $\gamma_1, \gamma_2, \gamma_3$, and ΔT , which extend the functionality of Adam. Among these, γ_1 and γ_2 serve a similar purpose to β_1 and β_2 in Adam, controlling the smoothness of updates to the first moment m_{norm} and the second moment v_{norm} . Larger values of γ_1 and γ_2 result in smoother updates, placing greater emphasis on historical gradient norm statistics when adapting the current gradient norm. Similarly, γ_3 plays a role in determining the threshold for identifying gradient spikes. A larger γ_3 leads to a smoother and more conservative threshold, resulting in a higher proportion of gradients being classified as spike gradients. To investigate the impact of these hyperparameters, we plot the final perplexity curve while varying γ_1 from 0.5 to 0.9, γ_2 from 0.8 to 0.999, γ_3 from 0.9 to 0.999, and ΔT from 250 to 5000. The experiments are conducted using LLaMA-60M, trained on 1.1B C4 tokens under the FP4 training setting. The results in Figure 8 demonstrate that overly small or excessively large values of these hyperparameters can degrade performance. However, the intuitive interpretations of these hyperparameters make them

straightforward to tune, and they typically require minimal adjustments. In this paper, we adopt the

optimal values $\gamma_1 = 0.7$, $\gamma_2 = 0.9$, $\gamma_3 = 0.999$, and $\Delta T = 1000$, which work effectively for all 4-bit training scenarios.

5 RELATED WORK

432

433

434 435 436

437 438

439

440

441

442

443

444

445

446

447

448

449

450

451

452

453

454

455

456 457

458 459

460

461

462

463

464

465

466

467

468

469

470

471

472

473

474

475 476

477 478 479

480

481

482

483

484

485

Instability of Training Large Language Models. The instability of large language model (LLM) training, which are marked by loss spikes and catastrophic divergence (Chowdhery et al., 2023; Molybog et al., 2023), has driven extensive research into stabilization techniques. These methods generally fall into three main categories: (1) gradient preprocessing, (2) architectural modifications, and (3) initialization strategies. Gradient preprocessing typically involves scaling and clipping gradients at the start of the optimization process to stabilize the training. A well-known example is gradient clipping (Goodfellow, 2016), which globally rescales the gradient norm to a fixed value. Later, Adafactor (Shazeer & Stern, 2018) introduced capping the norm of the parameter updates instead of the raw gradients. More recently, SPAM (Huang et al., 2025) proposed detecting and clipping anomalous gradients based on historical gradient statistics. However, a common drawback of these methods is that they require manually setting a predefined threshold. Architecturally, Xiong et al. (2020) showed that Post-LayerNorm (Post-LN) amplifies gradients, causing instability with large learning rates, while Pre-LayerNorm (Pre-LN) preserves gradient norms for stable training. Embed LayerNorm (Embed LN) normalizes embeddings (Dettmers et al., 2021), though it may impact performance (Scao et al., 2022), while Embed Detach (Ding et al., 2021; Zeng et al., 2022) reduces loss spikes by truncating gradients. DeepNorm (Wang et al., 2024) scales residual connections, and α Reparam (Zhai et al., 2023) prevents attention entropy collapse via spectral-normalized parameterization. Initialization strategies offer complementary stability benefits. Scaled Embed (Takase et al., 2023) stabilizes LayerNorm gradients, while Scaled Initialization (Nguyen & Salazar, 2019) reduces variance using $\mathcal{N}(0, \sqrt{2/(5d)}/\sqrt{2N})$. Fixup (Zhang et al., 2019; Huang et al., 2020) eliminates LayerNorm entirely, inspiring norm-free architectures. Though ongoing advancements refine these approaches, training stability remains a key challenge in LLM development.

Low-precision LLM Training. Low-precision training Wang et al. (2018); Lin et al. (2022); Xi et al. (2024a;b); Wortsman et al. (2023a) has emerged as a promising approach to improve both computational and memory efficiency during training. Among these methods, FP16 Micikevicius et al. (2017) and BF16 Kalamkar et al. (2019) are the most widely adopted precision formats. To push the efficiency further, 8-bit training has garnered increasing attention. For instance, LM-FP8 Peng et al. (2023) enables training with FP8 precision. While Fishman et al. (2024) demonstrates that as training scales up (larger than 250B tokens), the issue of activation outliers becomes more pronounced, posing challenges to the representation range of low-bit data formats. To address this challenge, Fishman et al. (2024) proposes a smoothing strategy, while Ashkboos et al. (2025) leverages Hadamard transformations to mitigate the impact of activation outliers. Furthermore, the choice of data format significantly influences training performance. The INT8 format is the most widely supported lowprecision format, whereas FP8, available in NVIDIA's Hopper GPU architecture, provides specialized support. Additionally, the MX format Rouhani et al. (2023) demonstrates superior representational capability, though it is rarely supported by current hardware. In this work, we investigate the training instability associated with low-precision training and propose enhancements through the design of optimizers. Our approach is compatible with existing techniques, providing a complementary solution to improve the stability of low-precision training.

6 Conclusion

This paper presents a comprehensive study on the training instability challenges of 4-bit quantization in large language models. We find that while low-precision training significantly reduces memory and computational costs, it also amplifies the sensitivity to learning rates, and increases the likelihood of gradient and loss spikes. To address these issues, we propose Stable-SPAM, an optimizer that combines three key techniques: AdaClip, AdaGN, and MoRet. Empirical results on LLaMA models of various sizes demonstrate that Stable-SPAM not only stabilizes 4-bit training but also achieves better performance compared to existing optimizers. We additionally show that these stabilization strategies are broadly applicable, benefiting other optimizers like Lion and Adam-mini.

7 ETHICS STATEMENT

This work fully complies with the ICLR Code of Ethics. All datasets employed in our study are publicly available and widely used in prior research. We have taken care to avoid any biases or discriminatory outcomes in our research process. No personally identifiable information was used, and no experiments were conducted that could raise privacy or security concerns. We are committed to maintaining transparency and integrity throughout the research process.

8 REPRODUCIBILITY STATEMENT

We provide comprehensive implementation details, including training procedures, evaluation protocols, and hyperparameter settings, in Section 4 and Appendix B. The source code has been made available for the review process and will be publicly released to support reproducibility and to facilitate future research.

REFERENCES

- Saleh Ashkboos, Mahdi Nikdan, Soroush Tabesh, Roberto L Castro, Torsten Hoefler, and Dan Alistarh. Halo: Hadamard-assisted lossless optimization for efficient low-precision llm training and fine-tuning. *arXiv preprint arXiv:2501.02625*, 2025.
- Xiangning Chen, Chen Liang, Da Huang, Esteban Real, Kaiyuan Wang, Hieu Pham, Xuanyi Dong, Thang Luong, Cho-Jui Hsieh, Yifeng Lu, et al. Symbolic discovery of optimization algorithms. *Advances in neural information processing systems*, 36, 2024.
- Aakanksha Chowdhery, Sharan Narang, Jacob Devlin, Maarten Bosma, Gaurav Mishra, Adam Roberts, Paul Barham, Hyung Won Chung, Charles Sutton, Sebastian Gehrmann, et al. Palm: Scaling language modeling with pathways. *Journal of Machine Learning Research*, 24(240):1–113, 2023.
- Tim Dettmers, Mike Lewis, Sam Shleifer, and Luke Zettlemoyer. 8-bit optimizers via block-wise quantization. *arXiv preprint arXiv:2110.02861*, 2021.
- Ming Ding, Zhuoyi Yang, Wenyi Hong, Wendi Zheng, Chang Zhou, Da Yin, Junyang Lin, Xu Zou, Zhou Shao, Hongxia Yang, et al. Cogview: Mastering text-to-image generation via transformers. *Advances in neural information processing systems*, 34:19822–19835, 2021.
- Maxim Fishman, Brian Chmiel, Ron Banner, and Daniel Soudry. Scaling fp8 training to trillion-token llms. *arXiv preprint arXiv:2409.12517*, 2024.
- Ian Goodfellow. Deep learning, 2016.
- Tianjin Huang, Ziquan Zhu, Gaojie Jin, Lu Liu, Zhangyang Wang, and Shiwei Liu. Spam: Spike-aware adam with momentum reset for stable llm training. *arXiv preprint arXiv:2501.06842*, 2025.
- Xiao Shi Huang, Felipe Perez, Jimmy Ba, and Maksims Volkovs. Improving transformer optimization through better initialization. In *International Conference on Machine Learning*, pp. 4475–4483. PMLR, 2020.
- Dhiraj Kalamkar, Dheevatsa Mudigere, Naveen Mellempudi, Dipankar Das, Kunal Banerjee, Sasikanth Avancha, Dharma Teja Vooturi, Nataraj Jammalamadaka, Jianyu Huang, Hector Yuen, et al. A study of bfloat16 for deep learning training. *arXiv preprint arXiv:1905.12322*, 2019.
- Diederik P Kingma. Adam: A method for stochastic optimization. *arXiv preprint arXiv:1412.6980*, 2014.
- Joonhyung Lee, Jeongin Bae, Byeongwook Kim, Se Jung Kwon, and Dongsoo Lee. To fp8 and back again: Quantifying the effects of reducing precision on llm training stability. *arXiv* preprint *arXiv*:2405.18710, 2024.

- Shenggui Li, Hongxin Liu, Zhengda Bian, Jiarui Fang, Haichen Huang, Yuliang Liu, Boxiang Wang, and Yang You. Colossal-ai: A unified deep learning system for large-scale parallel training. In *Proceedings of the 52nd International Conference on Parallel Processing*, pp. 766–775, 2023.
 - Vladislav Lialin, Sherin Muckatira, Namrata Shivagunde, and Anna Rumshisky. Relora: Highrank training through low-rank updates. In *The Twelfth International Conference on Learning Representations*, 2023.
 - Ji Lin, Ligeng Zhu, Wei-Ming Chen, Wei-Chen Wang, Chuang Gan, and Song Han. On-device training under 256kb memory. Advances in Neural Information Processing Systems, 35:22941– 22954, 2022.
 - Aixin Liu, Bei Feng, Bing Xue, Bingxuan Wang, Bochao Wu, Chengda Lu, Chenggang Zhao, Chengqi Deng, Chenyu Zhang, Chong Ruan, et al. Deepseek-v3 technical report. *arXiv preprint arXiv:2412.19437*, 2024.
 - Ilya Loshchilov and Frank Hutter. Decoupled weight decay regularization. *arXiv preprint arXiv:1711.05101*, 2017.
 - Chao Ma, Wenbo Gong, Meyer Scetbon, and Edward Meeds. Swan: Preprocessing sgd enables adam-level performance on llm training with significant memory reduction. *arXiv* preprint *arXiv*:2412.13148, 2024.
 - Paulius Micikevicius, Sharan Narang, Jonah Alben, Gregory Diamos, Erich Elsen, David Garcia, Boris Ginsburg, Michael Houston, Oleksii Kuchaiev, Ganesh Venkatesh, et al. Mixed precision training. *arXiv preprint arXiv:1710.03740*, 2017.
 - Igor Molybog, Peter Albert, Moya Chen, Zachary DeVito, David Esiobu, Naman Goyal, Punit Singh Koura, Sharan Narang, Andrew Poulton, Ruan Silva, et al. A theory on adam instability in large-scale machine learning. *arXiv preprint arXiv:2304.09871*, 2023.
 - Toan Q Nguyen and Julian Salazar. Transformers without tears: Improving the normalization of self-attention. *arXiv preprint arXiv:1910.05895*, 2019.
 - Yuqi Nie, Nam H Nguyen, Phanwadee Sinthong, and Jayant Kalagnanam. A time series is worth 64 words: Long-term forecasting with transformers. *arXiv preprint arXiv:2211.14730*, 2022.
 - Houwen Peng, Kan Wu, Yixuan Wei, Guoshuai Zhao, Yuxiang Yang, Ze Liu, Yifan Xiong, Ziyue Yang, Bolin Ni, Jingcheng Hu, et al. Fp8-lm: Training fp8 large language models. *arXiv preprint arXiv:2310.18313*, 2023.
 - Bita Darvish Rouhani, Ritchie Zhao, Ankit More, Mathew Hall, Alireza Khodamoradi, Summer Deng, Dhruv Choudhary, Marius Cornea, Eric Dellinger, Kristof Denolf, et al. Microscaling data formats for deep learning. *arXiv preprint arXiv:2310.10537*, 2023.
 - Teven Le Scao, Thomas Wang, Daniel Hesslow, Lucile Saulnier, Stas Bekman, M Saiful Bari, Stella Biderman, Hady Elsahar, Niklas Muennighoff, Jason Phang, et al. What language model to train if you have one million gpu hours? *arXiv preprint arXiv:2210.15424*, 2022.
 - Noam Shazeer. Glu variants improve transformer. arXiv preprint arXiv:2002.05202, 2020.
 - Noam Shazeer and Mitchell Stern. Adafactor: Adaptive learning rates with sublinear memory cost. In *International Conference on Machine Learning*, pp. 4596–4604. PMLR, 2018.
 - Sho Takase, Shun Kiyono, Sosuke Kobayashi, and Jun Suzuki. Spike no more: Stabilizing the pre-training of large language models. *arXiv preprint arXiv:2312.16903*, 2023.
 - Hugo Touvron, Louis Martin, Kevin Stone, Peter Albert, Amjad Almahairi, Yasmine Babaei, Nikolay Bashlykov, Soumya Batra, Prajjwal Bhargava, Shruti Bhosale, et al. Llama 2: Open foundation and fine-tuned chat models. *arXiv preprint arXiv:2307.09288*, 2023.
 - Hongyu Wang, Shuming Ma, Li Dong, Shaohan Huang, Dongdong Zhang, and Furu Wei. Deepnet: Scaling transformers to 1,000 layers. *IEEE Transactions on Pattern Analysis and Machine Intelligence*, 2024.

- Naigang Wang, Jungwook Choi, Daniel Brand, Chia-Yu Chen, and Kailash Gopalakrishnan. Training deep neural networks with 8-bit floating point numbers. *Advances in neural information processing systems*, 31, 2018.
 - Mitchell Wortsman, Tim Dettmers, Luke Zettlemoyer, Ari Morcos, Ali Farhadi, and Ludwig Schmidt. Stable and low-precision training for large-scale vision-language models. *Advances in Neural Information Processing Systems*, 36:10271–10298, 2023a.
 - Mitchell Wortsman, Peter J Liu, Lechao Xiao, Katie Everett, Alex Alemi, Ben Adlam, John D Co-Reyes, Izzeddin Gur, Abhishek Kumar, Roman Novak, et al. Small-scale proxies for large-scale transformer training instabilities. *arXiv preprint arXiv:2309.14322*, 2023b.
 - Haocheng Xi, Changhao Li, Jianfei Chen, and Jun Zhu. Training transformers with 4-bit integers. *Advances in Neural Information Processing Systems*, 36:49146–49168, 2023.
 - Haocheng Xi, Han Cai, Ligeng Zhu, Yao Lu, Kurt Keutzer, Jianfei Chen, and Song Han. Coat: Compressing optimizer states and activation for memory-efficient fp8 training. *arXiv preprint arXiv:2410.19313*, 2024a.
 - Haocheng Xi, Yuxiang Chen, Kang Zhao, Kai Jun Teh, Jianfei Chen, and Jun Zhu. Jetfire: Efficient and accurate transformer pretraining with int8 data flow and per-block quantization. *arXiv* preprint *arXiv*:2403.12422, 2024b.
 - Ruibin Xiong, Yunchang Yang, Di He, Kai Zheng, Shuxin Zheng, Chen Xing, Huishuai Zhang, Yanyan Lan, Liwei Wang, and Tieyan Liu. On layer normalization in the transformer architecture. In *International Conference on Machine Learning*, pp. 10524–10533. PMLR, 2020.
 - Aohan Zeng, Xiao Liu, Zhengxiao Du, Zihan Wang, Hanyu Lai, Ming Ding, Zhuoyi Yang, Yifan Xu, Wendi Zheng, Xiao Xia, et al. Glm-130b: An open bilingual pre-trained model. *arXiv preprint arXiv:2210.02414*, 2022.
 - Shuangfei Zhai, Tatiana Likhomanenko, Etai Littwin, Dan Busbridge, Jason Ramapuram, Yizhe Zhang, Jiatao Gu, and Joshua M Susskind. Stabilizing transformer training by preventing attention entropy collapse. In *International Conference on Machine Learning*, pp. 40770–40803. PMLR, 2023.
 - Biao Zhang and Rico Sennrich. Root mean square layer normalization. *Advances in Neural Information Processing Systems*, 32, 2019.
 - Hongyi Zhang, Yann N Dauphin, and Tengyu Ma. Fixup initialization: Residual learning without normalization. *arXiv* preprint arXiv:1901.09321, 2019.
 - Yushun Zhang, Congliang Chen, Ziniu Li, Tian Ding, Chenwei Wu, Yinyu Ye, Zhi-Quan Luo, and Ruoyu Sun. Adam-mini: Use fewer learning rates to gain more. *arXiv preprint arXiv:2406.16793*, 2024a.
 - Zhenyu Zhang, Ajay Jaiswal, Lu Yin, Shiwei Liu, Jiawei Zhao, Yuandong Tian, and Zhangyang Wang. Q-galore: Quantized galore with int4 projection and layer-adaptive low-rank gradients. *arXiv* preprint arXiv:2407.08296, 2024b.
 - Jiawei Zhao, Zhenyu Zhang, Beidi Chen, Zhangyang Wang, Anima Anandkumar, and Yuandong Tian. Galore: Memory-efficient llm training by gradient low-rank projection. arXiv preprint arXiv:2403.03507, 2024a.
 - Rosie Zhao, Depen Morwani, David Brandfonbrener, Nikhil Vyas, and Sham Kakade. Deconstructing what makes a good optimizer for language models. *arXiv preprint arXiv:2407.07972*, 2024b.

A THE USE OF LARGE LANGUAGE MODELS (LLMS)

Large Language Models (LLMs) were not involved in the development of the research methodology, experimental design, analyses, or original contributions of this work. Their use was strictly limited to general-purpose editorial assistance, including refining wording and improving readability.

The authors take full responsibility for the manuscript, including any text polished with LLM assistance. We have ensured that all usage complies with ethical guidelines and does not involve plagiarism, fabrication, or other forms of scientific misconduct.

B ARCHITECTURE AND HYPERPARAMETERS

We introduce details of the LLaMA architecture and hyperparameters used for 4-bit and BF16 pretraining, following Lialin et al. (2023); Zhao et al. (2024a). Table 6 shows the most hyperparameters of LLaMA models across model sizes. We use a max sequence length of 256 for all models, with a batch size of 512, with a batch size of 131K tokens. For all experiments, we adopt learning rate warmup of 2000 training steps, and use cosine annealing for the learning rate schedule, decaying to 10% of the initial learning rate.

Table 6: Configurations of LLaMA models used in this paper.

Params	Hidden	Intermediate	Heads	Layers
60 M	512	1376	8	8
130M	768	2048	12	12
350M	1024	2736	16	24
1 B	2048	5461	24	32

For all methods across each model size (from $60 \mathrm{M}$ to $7 \mathrm{B}$), we tune the learning rates from 1 e - 4 to 1 e - 3 with an increasing step of 2×10^{-4} for pre-training tasks, and the best learning rate is selected based on the validation perplexity. The detailed hyperparameter of <code>Stable-SPAM</code> on 4-bit training and BF16 training are reported in Table 7 and Table 8.

Table 7: Hyperparameters of Stable-SPAM for 4-bit pre-training experiments in this paper.

Hyper-Parameters	LLaMA-130M	LLaMA-350M	LLaMA-1B	LLaMA-7B
LR	1e-3	4e-4	2e - 4	2e-4
ΔT	1000	1000	1000	1000
γ_1	0.7	0.7	0.7	0.7
γ_2	0.9	0.9	0.9	0.9
γ_3	0.999	0.999	0.999	0.999

Table 8: Hyperparameters of Stable-SPAM for BF6 pre-training experiments in this paper.

Hyper-Parameters	LLaMA-60M	LLaMA-130M	LLaMA-350M	LLaMA-1B
		Standard P	retraining	
LR	1e - 3	8e - 4	4e - 4	2e - 4
ΔT	1000	1000	1000	1000
γ_1	0.85	0.85	0.85	0.85
γ_2	0.99999	0.99999	0.99999	0.99999
γ_3	0.999	0.999	0.999	0.999

BROADER IMPACT

702

703

This paper advances the field of large language model (LLM) training by proposing a stable optimizer that enables more stable and efficient optimization at low-precision (4-bit) arithmetic. By reducing computational and memory overhead, our approach has the potential to lower energy consumption and lessen the environmental footprint of training large-scale models. There are many potential societal consequences of our work, none of which we feel must be specifically highlighted here.

709 710

711

EVALUATION ON FINE-TUNING TASK

712 713 714

We further evaluate Stable-SPAM on fine-tuning tasks using the pre-trained LLaMA2-7B model on the CommonsenseQA benchmark.

715

Table 9: Fine-tuning performance of LLaMA2-7B on various downstream tasks (CommenseQA). The rank for LoRA is set to 8.

716 717 718

719

722

723

724

725

Method	BoolQ	PIQA	SIQA	HellaSwag	WinoGrande	ARC-e	ARC-c	OBQA	Avg.
Adam	76.06	79.00	33.21	59.94	79.87	77.82	46.76	34.40	60.88
StableSPAM	77.92	78.89	33.52	60.10	80.43	77.78	47.70	34.80	61.39

720 721

The results in Table 9 demonstrate that StableSPAM outperforms Adam during fine-tuning with LoRA. However, the performance improvements are less pronounced than those observed in the pre-training setting. We attribute this to the characteristics of fine-tuning tasks, which typically employ much smaller learning rates (e.g., 5e-5 in our experiments). A plausible explanation is that smaller learning rates inherently suppress the occurrence of gradient and loss spikes, thereby diminishing the relative advantage of StableSPAM.

726 727 728

Е EXPERIMENTS COMPUTE RESOURCES

729 730 731

All experiments are conducted using NVIDIA H100 GPUs. LLaMA-60M, 130M, and 350M models are trained with 2 H100 GPUs, while the LLaMA-1B model is trained with 4 H100 GPUs.

732 733 734

EFFECT OF REDUCING GRADIENT NORM SPIKES

735 736 737

We introduce a spike-counting metric based on gradient norm deviations. Specifically, a spike is defined via the z-score:

738 739

$$z_{\text{score}} = \frac{g_t - \mu_t}{\delta_t}$$

740

741

742

where μ_t and δ_t are the rolling mean and standard deviation over a window of K=100 steps and g_t is the gradient norm at step t. A spike is recorded whenever the z-score exceeds a fixed threshold (typically 5).

743 744 745

The Table 10 reports the total number of spikes and final perplexity for FP32, BF16, and FP4 training using Adam and Stable-SPAM, evaluated on LLaMA-350M with 2.2B tokens: We observed:

746 747

• The number of spikes increases significantly as precision decreases;

748 749 • Stable-SPAM effectively suppresses gradient norm spikes in FP4 training, reducing them to levels comparable to—or even lower than—those observed with Adam under BF16 training, yielding better final perplexity.

750 751 752

RUNTIME AND MEMORY COST

753 754

755

We measured both the wall-clock time per 100 training steps and the peak optimizer memory usage for LLaMA-130M and LLaMA-350M, trained on a single NVIDIA H100 GPU. As shown in Table 11 and Table 12, the computational and memory overhead introduced by Stable-SPAM compared to

Table 10: #Spikes of gradient norm for Adam and Stable-SPAM during training process

	FP32(Adam)	BF16 (Adam)	FP4 (Adam)	FP4 (Stable-SPAM)
#Spikes	9	32	60	26
Final Perplexity	19.301	21.38	24.59	19.49

Adam is negligible. This confirms that the proposed optimizations in Stable-SPAM incur minimal burden in terms of compute and bandwidth.

Table 11: Runtime of 100 steps for training LLaMA-130M and 350M based on 1 Nvidia H100 GPU

	LLaMA-130M	LLaMA-350M
Adam	219 (s)	543 (s)
StableSPAM	222(s)	548 (s)

Table 12: GPU memory usage of optimizer for training LLaMA-130M and 350M

	LLaMA-130M	LLaMA-350M
Adam	842.59 (M)	2187.3 (M)
StableSPAM	849.1 (M)	2203.81 (M)

H ADDITIONAL EXPERIMENTS ON OTHER TASKS

To further validate its general applicability beyond language modeling, we conducted additional experiments on reinforcement learning (MuJoCo) and time series forecasting (weather prediction) tasks,

H.1 REINFORCEMENT LEARNING TASK

As shown in Table 13, Stable-SPAM consistently outperforms Adam on the HalfCheetah, Walker2d, and Ant environment, highlighting its effectiveness across diverse reinforcement learning tasks.

H.2 TIME SERIES FORESCASTING TASK

We conducted additional experiments on time-series prediction tasks. In these experiments, we intentionally introduced anomalous data with a probability A=10% to simulate gradient anomalies. Experiments are conducted with 10 repeated runs on Weather time series data³ using PatchTST (Nie et al., 2022) model. The results are presented in Figure 9.

The findings demonstrate that as the severity (S) of anomalous data increases, Stable-SPAM's performance advantage over Adam becomes more pronounced. Besides, Stable-SPAM consistently surpasses SPAM across all settings. These results further highlight the effectiveness of the proposed Stable-SPAM.

I PSEUDOCODE

The pseudocode is presented in Alogrithm 1.

³https://www.bgc-jena.mpg.de/wetter/

Table 13: The final Test Rewards for the three mujoco environment: HalfCheetah, Walker2d and Ant.

	HalfCheetah	Ant	Hopper
Adam	5276.1 ± 1542.9	3835.6 ± 759.5	2447.5 ± 1037.9
StableSPAM	6762.6 ± 1414.2	4907.6 ± 954.6	3435.1 ± 1178.3

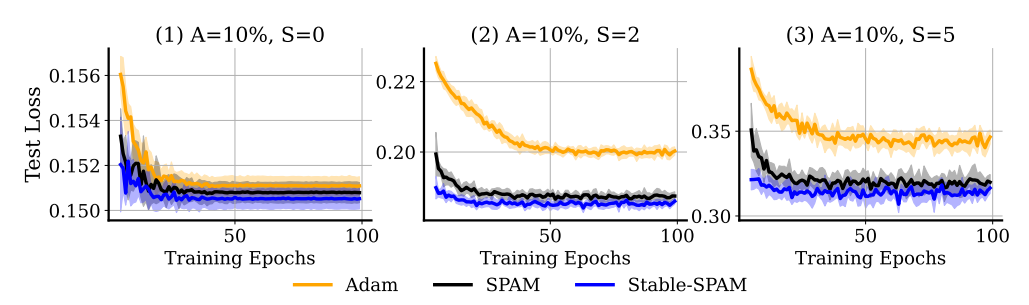


Figure 9: Test Loss during Training Process on Weather Time-series Data. Anomalous data is generated by adding Gaussian noise to 10% of randomly selected input values. Specifically, the anomalies data are conducted with X = X + Gaussin(0, Severity * Max(X)) where X is the inputs and S is the severity.

Algorithm 1: Stable-SPAM

```
Input: A layer weight matrix w \in \mathbb{R}^{m \times n}, learning rate \alpha, decay rates \beta_1 = 0.9, \beta_2 = 0.999, initial
            parameters w_0, \gamma_1=0.7, \gamma_2=0.9 for AdaGN and \gamma_3=0.999 for AdaClip, momentum reset interval \Delta T, small constant \epsilon=1\times 10^{-6}, and total training steps T.
```

Output: Optimized parameters w_T .

```
835
               {\bf 1} \ \ {\bf while} \ t < T \ {\bf do}
                                   g_t \in \mathbb{R}^{m \times n} \leftarrow -\nabla_w \phi_t(w_t)
                                                                                                                             // Gradient of the objective at step t. \,
836
               2
                                    g_{\max} \leftarrow \text{Max}(\text{abs}(g_t))
               3
837
                                   T_{\text{threshold}} \leftarrow T_{\text{threshold}} \cdot \theta + (1 - \theta) g_{\text{max}}
               4
838
                                   \widehat{T}_{\text{threshold}} \leftarrow \frac{T_{\text{threshold}}}{1 - \theta^t}
839
                                                                                                                                                  // Bias correction for threshold
                5
840
                                   \operatorname{Mask}_{\operatorname{spikes}} \leftarrow (\operatorname{abs}(g_t) > \widehat{T}_{\operatorname{threshold}})
                                  \begin{aligned} \operatorname{Mask_{spikes}} &\leftarrow (\operatorname{abs}_{spike}), \\ & \operatorname{if} \operatorname{sum}(\operatorname{Mask_{spikes}}) > 0 \operatorname{then} \\ & g_t[\operatorname{Mask_{spikes}}] \leftarrow \frac{g_t[\operatorname{Mask_{spikes}}]}{g_{\max}} \times \widehat{T}_{\operatorname{threshold}} \end{aligned}
841
842
843
844
                                   g_{\text{norm}} \leftarrow \|g_t\|_2
845
                                   m_{\text{norm}} \leftarrow \gamma_1 m_{\text{norm}} + (1 - \gamma_1) g_{\text{norm}}
              10
                                   \begin{aligned} v_{\text{norm}} &\leftarrow \gamma_2 \, v_{\text{norm}} + (1 - \gamma_2) \, g_{\text{norm}}^2 \\ \widehat{m}_{\text{norm}} &\leftarrow \frac{m_{\text{norm}}}{1 - \gamma_1^t}, \, \widehat{v}_{\text{norm}} \leftarrow \frac{v_{\text{norm}}}{1 - \gamma_2^t} \end{aligned}
846
              11
847
                                                                                                                                                  // Bias-corrected norm estimates
              12
848
                                   adaptive_norm \leftarrow -
849
              13
                                                                                \sqrt{\widehat{v}_{\mathrm{norm}}} + \epsilon
850
                                   g_t \leftarrow \frac{g_t}{g_t} \times \text{adaptive\_norm}
              14
851
                                   if (Mod(t, \Delta T) = 0) then
852
              15
                                                 m \leftarrow \text{zeros\_like}(m)
              16
853
                                                 v \leftarrow \texttt{zeros\_like}(v)
              17
854
                                   \boldsymbol{m}_t \leftarrow \beta_1 \, \boldsymbol{m}_{t-1} + (1 - \beta_1) \, g_t
              18
855
                                    \boldsymbol{v}_t \leftarrow \beta_2 \, \boldsymbol{v}_{t-1} + (1 - \beta_2) \, g_t^2
              19
856
                                                                                                                                  // bias correction
857
             20
                                                    \frac{1-\beta_1^t}{\boldsymbol{v}_t}
858
                                                                                                                                 // bias correction
             21
859
              22
861
                                   t \leftarrow t + 1
             23
862
             24 return w_T.
```